Arbitrary Configuration Stabilization Control for Nonholonomic Vehicle with Input Saturation

Arbitrary Configuration Stabilization Control for Nonholonomic Vehicle With Input Saturation: A c-Nonholonomic Trajectory Approach

Xiuhui Peng, Zhiyong Sun, *Member, IEEE*, Mou Chen, *Senior Member, IEEE*, and Zhiyong Geng

***Abstract*—This article addresses the saturated stabilization control problem for nonholonomic vehicles with a novel c-nonholonomic trajectory approach on SE(2), with applications to automatic parking. First, by defining the c-nonholonomic configuration, a c-nonholonomic trajectory is obtained, which provides a novel approach to design stabilization controller to reach an arbitrary configuration. Second, a global discontinuous time-invariant feedback controller with input saturation is proposed, which does not involve time signal information, and its convergence is illustrated by a Lyapunov function approach. Thereafter, the motion trajectory of the proposed controller is analyzed, and the application scenario in automatic parking with the approximate desired trajectory is demonstrated. Finally, the performance of the proposed controller is validated by both numerical simulations and experiments.**

***Index Terms*—Arbitrary configuration stabilization, automatic parking, c-nonholonomic trajectory approach, nonholonomic vehicle.**

I. Introduction

DUE to the nonholonomic constraint, even though the tracking control problem has been extensively studied under the persistence of excitation condition of reference velocity [1]–[4], the arbitrary configuration stabilization control problem for nonholonomic vehicle is always an open issue, which is hard to solve in the past several decades [5]. In particular, by taking some desired properties into account, such as maintaining the time-invariant feedback controller without involving time signal t, input saturation, moving along an approximate desired trajectory, the related stabilization control results are very rare. In this article, based on a new c-nonholonomic configuration approach, a novel global discontinuous time-invariant feedback control law is proposed to solve the stabilization problem with input saturation and approximate desired trajectory.

The difficulty in arbitrary configuration stabilization control for nonholonomic vehicle comes from that the vehicle cannot have lateral movement due to the underactuated property. Based on the Brockett's theorem [5], it is well known that it is impossible to find a smooth or continuous feedback stabilization control law to stabilize the configuration of nonholonomic vehicles, and the existing stabilization control laws can be classified into the smooth time-varying feedback [6]–[9], discontinuous time-invariant feedback [10]–[12], hybrid feedback [13]–[15], transverse function approach [16], among others.

Recently, some significant advances on designing stabilization controller for nonholonomic vehicles are reported in the literature [19]–[22], [24]–[27]. Considering the input saturation and external disturbances in [19], a smooth time-varying feedback control is proposed by designing a new auxiliary angle to solve the stabilization and tracking control problem. Based on the Lyapunov approach, the simultaneous stabilization and tracking control problem is solved in [20] and [21] by designing a delicate time-varying signal in the attitude control loop, and then the robust stabilization and formation problem is addressed with a smooth time-varying feedback controller in [22]. Inspired by the field lines and equipotential lines of electric dipole, a vector field approach is proposed to solve the stabilization control problem for underactuated marine vehicle in [23]. From the point of view of stabilizing fully-actuated vehicles, a variable angle between the direction of y-linear speed and that of x-linear speed for fully-actuated vehicle is proposed to add the attitude loop so that the stabilization control problem is solved in [24]. Then, its kinematics controller has been extended to the dynamical controller in [25] with a prespecified time convergence. Furthermore, some of relevant and significant research works are proposed in [26] and [27], and reference therein.

After summarizing the existing literature on stabilization control of nonholonomic vehicle, there still exists several aspects

Manuscript received October 15, 2020; revised October 28, 2020 and December 23, 2020; accepted February 3, 2021. Date of publication February 25, 2021; date of current version October 27, 2021. This work was supported in part by the National Natural Science Foundation of China under Grant 61773024, in part by the Natural Science Foundation of Jiangsu Province of China under Grant BK20200438, in part by the China Postdoctoral Science Foundation under Grant 2020TQ0150 and Grant 2020M671482. *(Corresponding author: Mou Chen.)*

Xiuhui Peng and Mou Chen are with the College of Automation Engineering, Nanjing University of Aeronautics, and Astronautics, Nanjing 211106, China (e-mail: xhpeng@nuaa.edu.cn; chenmou@nuaa.edu.cn).

Zhiyong Sun is with the Department of Electrical Engineering, Eindhoven University of Technology, Eindhoven 5612, The Netherlands (e-mail: sun.zhiyong.cn@gmail.com).

Zhiyong Geng is with the State Key Laboratory for Turbulence and Complex Systems, Department of Mechanics and Engineering Science, College of Engineering, Peking University, Beijing 100871, China (e-mail: zygeng@pku.edu.cn).

This article has supplementary material provided by the authors and color versions of one or more figures available at https://doi.org/10.1109/TIE.2021.3060674.

Digital Object Identifier 10.1109/TIE.2021.3060674

that should be further improved. Firstly, most existing stabilization control laws require the information of time t at all-time instants, such as [19]–[22], [26], [27]. However, real vehicles are often equipped with digital systems, which in general do not have enough memory units in advanced RISC machines or digital signal processors. Even if certain vehicles have the memory unit installed, an instantaneous loss of power will cause the clock to reset which is not suitable for real-time practical realization. Therefore, solving controller equations independent of time signal t is highly preferable for engineering implementation. Thus, it is very important to design a stabilization controller with a novel time-invariant state feedback, which does not contain time signal t in the control function. Secondly, an important issue arising from the practical application is input saturation. Even if the stabilization controller proposed in [24] and [25] does not contain the time signal t, it cannot realize the task when input saturation is considered. From both theoretical and practical points of view, the development of a novel control law with input saturation is a significant task due to the limitation of the speeds brought by vehicle's motor [28]. As far as we know, the discontinuous time-invariant state feedback control law with input saturation is rarely studied in the existing literature. Thirdly, most existing stabilization controllers only realize the goal of stabilization for nonholonomic vehicles, but the motion trajectories from an initial configuration to a desired configuration under those control laws are not considered. For example, an important application scenario of stabilization control law is the automatic parking, which requires the simultaneous desired position and attitude stabilization. Therefore, designing a novel controller that is able to calculate the motion trajectory (an approximate desired trajectory) in advance remains open to be solved.

As is known to all, it is an open problem to design a novel discontinuous time-invariant state feedback control law that considers both input saturation and approximate desired trajectory for nonholonomic vehicles. To solve this problem, the properties of nonholonomic vehicles should be explored thoroughly. In this article, some original concepts for nonholonomic vehicles are studied, based on which a novel approach is then developed to solve the arbitrary configuration stabilization control problem. By designing a c-nonholonomic configuration, a novel c-nonholonomic trajectory approach is proposed. Based on the novel c-nonholonomic approach, the saturated controller and its application scenario in automatic parking are studied. To summarize, the main contributions of this article are listed as follows.

1) A novel c-nonholonomic trajectory approach is proposed to solve the arbitrary configuration stabilization problem for nonholonomic vehicles on SE(2). By defining the c-nonholonomic configuration, the c-nonholonomic trajectory is realized. To the best of our knowledge, it is the first time that such a c-nonholonomic trajectory approach is studied that solves the stabilization control problem of nonholonomic vehicles.
2) Based on the c-nonholonomic trajectory approach, the proposed controller could guarantee the input saturation on the designed linear and angular speed. Meanwhile, the proposed controller maintains a novel global discontinuous time-invariant state feedback form so that the controller does not involve additional memory to calculate the time signal t. Thus, the proposed control law is more suitable for implementation in practice.
3) The motion trajectory of vehicle under the proposed controller can be determined in advance, and the automatic parking application scenario with the approximate desired trajectory is achieved under the proposed controller.

The remainder of this article is structured as follows. The notations and problem formulation are introduced in Section II. The c-nonholonomic configuration and c-nonholonomic trajectory are presented in Section III. Section IV introduces the saturated controller and its analysis on motion trajectory. Simulation and experiment results are shown in Section V. Finally, Section VI concludes this article.

II. Background and Problem Formulation

A. Notations

Some notations are first given here. The symbol Z represents an integer. Denote e_1, e_2 as the natural bases of $\mathbb{R}^2$. Let $\mathcal{F}_B$ be the body-fixed frame, which is the principal axes of the rigid body attached to the vehicle's center of mass. $\mathcal{F}_I$ represents the inertial frame. Following the conventions in the literature (e.g., [10]), we define $\arctan(0/0) = 0$, $\arctan(y/0) = \pi/2$ for $y \neq 0$.

In this article, the special Euclidean group $\mathrm{SE}(2)$ is employed to describe the configuration space of a planar vehicle with two dimensions [30]. The group element $g \in \mathrm{SE}(2)$, representing the configuration space globally and uniquely, is denoted by

$$g = \begin{bmatrix} R & p \\ 0 & 1 \end{bmatrix} = \begin{bmatrix} \cos\theta & -\sin\theta & x \\ \sin\theta & \cos\theta & y \\ 0 & 0 & 1 \end{bmatrix}$$

where $p \in \mathbb{R}^2$ represents the position of a rigid body in the internal frame $\mathcal{F}_I$. For a given $g \in \mathrm{SE}(2)$, $g(m,n)$ represents element in the mth row and nth column of the matrix g, where $m = 1, 2, 3$, and $n = 1, 2, 3$. Special orthogonal group is denoted as $\mathrm{SO}(2) := \{R \in \mathbb{R}^{2\times 2} : R^T R = I_2, \det(R) = 1\}$, and $R \in \mathrm{SO}(2)$ describes the orientation from $\mathcal{F}_B$ to $\mathcal{F}_I$. It is important to point out that, for a given $R \in \mathrm{SO}(2)$, there exists a unique corresponding heading angle $\theta \in (-\pi, \pi]$. For convenience, we denote $g \in \mathrm{SE}(2)$ occasionally as $g \triangleq (\theta, x, y)$.

The tangent space of special Euclidean group $\mathrm{SE}(2)$ at the identity is denoted as Lie algebra $\mathfrak{se}(2)$. The Lie algebra element $\hat{\xi} \in \mathfrak{se}(2)$ represents the velocity of a vehicle in the body-fixed frame $\mathcal{F}_B$, and is denoted by

$$\hat{\xi} = \begin{bmatrix} \hat{\omega} & \nu \\ 0 & 0 \end{bmatrix} = \begin{bmatrix} 0 & -\omega & \nu_x \\ \omega & 0 & \nu_y \\ 0 & 0 & 0 \end{bmatrix}$$

where $\xi = [\omega, \nu_x, \nu_y]^T \in \mathbb{R}^3$, in which $\nu \in \mathbb{R}^2$ represents the translational speed, and $\omega \in \mathbb{R}$ (i.e., $\hat{\omega} \in \mathfrak{so}(2)$) is the angular speed. The map $(\cdot)^\wedge : \mathbb{R} \to \mathfrak{so}(2)$ represents the hat map, where $\mathfrak{so}(2) := \{\hat{x} \in \mathbb{R}^{2\times 2} | \hat{x}^T = -\hat{x}\}$. The inverse map of hat map is denoted as vee hap $(\cdot)^\vee : \mathfrak{so}(2) \to \mathbb{R}$. For two elements in Lie algebra $\hat{x} \in \mathfrak{se}(2)$ and $\hat{y} \in \mathfrak{se}(2)$, the Lie bracket is defined as

$[\hat{x},\hat{y}]=\hat{x}\hat{y}-\hat{y}\hat{x}$, and $\mathrm{ad}_{\hat{x}}^{i+1}\hat{y}=[\hat{x},\mathrm{ad}_{\hat{x}}^{i}\hat{y}]$ is the iterative Lie bracket, where $\mathrm{ad}_{\hat{x}}^{0}\hat{y}=\hat{y}$, and $i=0,1,\ldots,n$.

A planar rigid body in kinematic level is said to satisfy the nonholonomic constraint if the equation $-\dot{x}\sin\theta+\dot{y}\cos\theta=0$ holds. In this case, the velocity ξ satisfies $\nu_y=0$. In this article, we let $v\triangleq\nu_x$ denote the linear speed of the nonholonomic vehicles.

B. Problem Description

Consider the vehicle subject to nonholonomic constraint, and its equation of motion is modeled as

$$\dot{p}=vRe_1 \tag{1a}$$

$$\dot{R}=R\hat{\omega} \tag{1b}$$

where $R\in\mathrm{SO}(2)$ with the heading angle $\theta\in(-\pi,\pi]$. Considering the physical velocity constraints in practice, the following limited inputs are given as:

$$-v_m\le v\le v_m,\quad -\omega_m\le\omega\le\omega_m \tag{2}$$

where $v_m\in\mathbb{R}^+$ and $\omega_m\in\mathbb{R}^+$ are the known maximum allowable linear speed and angular speed.

We denote $g_d\in\mathrm{SE}(2)$ as the desired configuration. The main objective of this article is to find a stabilization control law to solve the arbitrary configuration stabilization problem with input saturation, so that the appropriate velocity input (v,ω), which satisfies the saturated input (2) for nonholonomic vehicle (1) is designed to realize the arbitrary configuration stabilization task, i.e., $g_d^{-1}g\to I_3$. Meanwhile, the application scenario in the automatic parking is analyzed with the proposed control method.

III. C-Nonholonomic Trajectory Approach

To solve the arbitrary configuration stabilization control problem for nonholonomic planar vehicles with input saturation and approximate desired trajectory, the c-nonholonomic trajectory approach is proposed firstly in this section.

We first introduce the exponential map and logarithm map on $\mathrm{SE}(2)$. For a given matrix $A\in\mathbb{R}^{n\times n}$, the exponential map on A is defined as $\exp A=\sum_{k=0}^{+\infty}\frac{A^k}{k!}$, where $\mathbb{R}^{n\times n}\to\mathbb{R}^{n\times n}$. In the special Euclidean group $\mathrm{SE}(2)$, it has an explicit form [30]. For the given $\hat{\theta}\in\mathfrak{so}(2)$, $q\in\mathbb{R}^2$, and $\hat{X}=(\hat{\theta},q)\in\mathfrak{se}(2)$, the exponential map is denoted as

$$g=\exp\hat{X}=\begin{bmatrix}\exp\hat{\theta} & \mathcal{A}(\theta)q\\ 0 & 1\end{bmatrix}\in\mathrm{SE}(2) \tag{3}$$

where

$$\exp\hat{\theta}=\begin{bmatrix}\cos\theta & -\sin\theta\\ \sin\theta & \cos\theta\end{bmatrix},\mathcal{A}(\theta)=\begin{bmatrix}\frac{\sin\theta}{\theta} & -\frac{(1-\cos\theta)}{\theta}\\ \frac{(1-\cos\theta)}{\theta} & \frac{\sin\theta}{\theta}\end{bmatrix}.$$

The inverse of the exponential map is termed the *logarithm* map, and is defined as

$$\hat{X}=\log g=\begin{bmatrix}\hat{\theta} & \mathcal{A}^{-1}(\theta)p\\ 0 & 0\end{bmatrix}\in\mathfrak{se}(2) \tag{4}$$

where $g=(R(\theta),p)\in\mathrm{SE}(2)$ with $\mathrm{tr}(g)\neq-1$, and

$$\mathcal{A}^{-1}(\theta)=\begin{bmatrix}(\theta/2)\cot(\theta/2) & \theta/2\\ -\theta/2 & (\theta/2)\cot(\theta/2)\end{bmatrix}.$$

In the context of nonholonomic constraint, exponential map, and logarithm map, the concept of c-nonholonomic configuration is proposed as follows.

Definition 1: For a given constant scalar $c\neq0$, the subset of $\mathrm{SE}(2)$ is defined by

$$\begin{aligned}\mathcal{G}_c\triangleq\{g_c\in\mathrm{SE}(2)\mid\ & g_c(1,3)=cg_c(2,1)\\ & g_c(2,3)=c(1-g_c(1,1))\}\end{aligned} \tag{5}$$

is called a c-nonholonomic configuration.

From the definition, one can check that $\mathcal{G}_c$ is a Lie subgroup of $\mathrm{SE}(2)$. Meanwhile, the following properties of c-nonholonomic configuration hold.

Proposition 1: For any $g_c,q_c\in\mathcal{G}_c$, it holds that $g_c^{-1}\in\mathcal{G}_c$ and $g_cq_c\in\mathcal{G}_c$. In particular, $I_3\in\mathcal{G}_c$.

Proof: For each $g_c\in\mathcal{G}_c$, its inverse is obtained as follows:

$$g_c^{-1}=\begin{bmatrix}g_c(1,1) & g_c(2,1) & -cg_c(2,1)\\ -g_c(2,1) & g_c(1,1) & c(1-g_c(1,1))\\ 0 & 0 & 1\end{bmatrix}.$$

From this, one concludes that $g_c^{-1}\in\mathcal{G}_c$ holds.

For any $g_c,q_c\in\mathcal{G}_c$, it can be verified that $g_cq_c\in\mathcal{G}_c$ holds by matrix operations.

Based on the definition of $\mathrm{SE}(2)$, one has $I_3\in\mathrm{SE}(2)$. Thus, one obtains that $g_c(1,3)=cg(2,1)=0$, $g_c(2,3)=c(1-g_c(1,1))=0$ from $g_c(1,1)=1,g_c(2,1)=0$, which shows that $I_3\in\mathcal{G}_c$. ■

For a given nonholonomic unicycle-type ground vehicle, its current configuration may not satisfy the c-nonholonomic configuration. Thus, the following Lemma introduces the construction of a c-nonholonomic configuration.

Lemma 1: For a general configuration

$$g=\begin{bmatrix}R(\theta) & \begin{bmatrix}x\\ y\end{bmatrix}\\ 0_{1\times2} & 1\end{bmatrix}\in\mathrm{SE}(2) \tag{6}$$

where $x,y\neq0$, the c-nonholonomic configuration $g_c\in\mathcal{G}_c$ is constructed as follows:

$$g_c=\begin{bmatrix}R(\theta_c) & \begin{bmatrix}x\\ y\end{bmatrix}\\ 0_{1\times2} & 1\end{bmatrix}\in\mathrm{SE}(2) \tag{7}$$

where the angle θ_c satisfies $\tan\frac{\theta_c}{2}=\frac{y}{x}$, and the constant scalar $c=\frac{y}{1-\cos\theta_c}$.

Proof: From Definition 1 and $c=\frac{y}{1-\cos\theta_c}$, one can check that $g_c(2,3)=c(1-g_c(1,1))=y$ holds in (7). On the other hand, one has $g_c(1,3)=cg_c(2,1)=\frac{y}{1-\cos\theta_c}\sin\theta_c=\frac{y}{\tan\frac{\theta_c}{2}}=x$. Thus, the constructed subset in (7) is a c-nonholonomic configuration. ■

After constructing the c-nonholonomic configuration, the next issue is to find the relationship between the c-nonholonomic configuration $\mathcal{G}_c$ and the Lie algebra. In the light of exponential

map, the following Lemma gives the constructed $g_c \in \mathcal{G}_c$ from a Lie algebra.

Lemma 2: For the well-constructed $g_c \in \mathcal{G}_c$ in (7), its exponential map can be derived as

$$g_c = \exp\{(\xi_c)^\wedge\} \tag{8}$$

where $\xi_c = [\theta_c, c\theta_c, 0]^T \in \mathbb{R}^3$, and $(\xi_c)^\wedge \in \mathfrak{se}(2)$.

Proof: Let us examine the structure of Lie algebra of $g_c \in \mathcal{G}_c$

$$\log_{\mathrm{SE}(2)} g_c = \begin{bmatrix} 0 & -\theta_c & (\theta_c/2)(x\cot\frac{\theta_c}{2} + y) \\ \theta_c & 0 & 0 \\ 0 & 0 & 0 \end{bmatrix}$$

where the equation $\tan\frac{\theta_c}{2} = \frac{y}{x}$ is used. Noting that $x = c\sin\theta_c$ and $y = c(1-\cos\theta_c)$ in Lemma 1, one obtains

$$\begin{aligned} x\cot\frac{\theta_c}{2} + y &= \frac{x^2}{y} + y = c\left(\frac{\sin^2\theta_c}{1-\cos\theta_c} + 1 - \cos\theta_c\right) \\ &= \frac{c}{1-\cos\theta_c}(\sin^2\theta_c + 1 - 2\cos\theta_c + \cos^2\theta_c) \\ &= \frac{c}{1-\cos\theta_c}2(1-\cos\theta_c) = 2c \end{aligned}$$

which implies that constant scalar c can be obtained from the position (x, y), such that $c = \frac{x^2+y^2}{2y}$. Thus, the exponential coordinate of g_c can be rewritten as

$$\log_{\mathrm{SE}(2)} g_c = \begin{bmatrix} 0 & -\theta_c & c\theta_c \\ \theta_c & 0 & 0 \\ 0 & 0 & 0 \end{bmatrix} = (\xi_c)^\wedge$$

which implies that (8) holds. ■

The following result is a consequence of Lemma 2.

Lemma 3: If the closed-loop system of $g_c \in \mathcal{G}_c$ in (7) is designed as follows:

$$\dot{g}_c(t) = g_c(t)(-\xi_c(t))^\wedge \tag{9}$$

with the constant scalar $c = (x(0)^2 + y(0)^2)/(2y(0))$ and $y(0) \neq 0$, then the trajectory of $g_c(t)$ is a circle with the center of $(0, c)$ and the radius of c. Meanwhile, the c-nonholonomic configuration g_c can be stabilized to converge to the identity matrix I_3.

Proof: Let us denote $\hat{x}_c = \log g_c \in \mathfrak{se}(2)$. Based on the differential of exponential theorem in [31], one has $\dot{\hat{x}}_c = \sum_{k=0}^{\infty} \frac{B_k}{k!}\mathrm{ad}^k_{-\hat{x}_c}(-\dot{\hat{\xi}}_c)$, where $B_k, k = 0, \ldots, \infty$ are the Bernoulli numbers [32]. In light of $\xi_c(1,3)/\omega_c(2,1) = c$, one obtains that $\sum_{k=1}^{\infty} \frac{B_k}{k!}\mathrm{ad}^k_{-\hat{x}_c}(-\dot{\hat{\xi}}_c) = 0$, and $\dot{\hat{x}}_c$ can be rewritten as $\dot{\hat{x}}_c = -\dot{\hat{\xi}}_c$. Thus, the solution of (9) is expressed as $g_c(t) = g_c(0)\exp\{\int_0^t(-\xi_c)^\wedge dt\} = g_c(0)\exp\{\int_0^t(\xi_c)^\wedge dt\}^{-1}$. One can verify that $\bar{g}_c(t) := \exp\{\int_0^t(\xi_c)^\wedge dt\} \in \mathcal{G}_c$. Hence, it follows that $g_c(t) = g_c(0)\bar{g}_c^{-1}(t)$. Based on Proposition 1, one concludes that the trajectories satisfy $g_c(t) \in \mathcal{G}_c$ for all time, and the equations $x(t) = c\sin\theta_c(t)$ and $y(t) = c(1-\cos\theta_c(t))$ hold, which indicate that all trajectories always stay on the circle $x(t)^2 + (y(t)-c)^2 = c^2$.

For the attitude loop, we can see that the angle dynamics $\dot{\theta}_c(t) = -\theta_c(t)$ converges to zero under the angular velocity feedback $\omega = -\theta_c(t)$. Therefore, the nonholonomic vehicle can be stabilized to the original point with the angle $\theta_c = 0$, and the current linear velocity $v = -c\theta_c(t)$ equals zero, which implies the stabilization problem is solved. ■

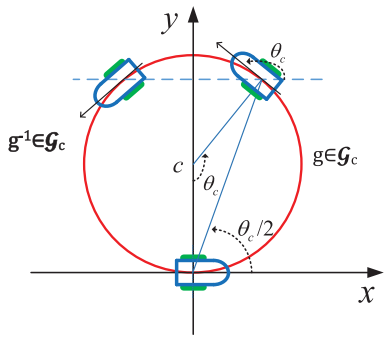

Fig. 1. c-nonholonomic trajectories.

Based on the abovementioned analysis, the definition of c-nonholonomic trajectory is presented as follows.

Definition 2: The trajectory generated by the system (9) is named as the c-nonholonomic trajectory.

Remark 1: From the analysis of Lemmas 1 and 2, one concludes that the c-nonholonomic trajectory can be generated by the linear speed $-c\theta_c(t)$ and angular speed $-\theta_c(t)$ if the initial configuration satisfies Definition 1. A c-nonholonomic trajectory is shown in Fig. 1 , which implies that its radius is the constant scalar c. From this point of view, the c-nonholonomic trajectory approach is also called the adjoint-circular-trajectory approach. Furthermore, note that the trajectory generated by (9) involves a time-varying speed motion, and the velocity converges to zero as the configuration approaches the desired configuration.

After presenting the c-nonholonomic trajectory, the next important issue is how to design the arbitrary configuration stabilization controller by using the ideas of the proposed c-nonholonomic trajectory, since the initial configuration of a vehicle may not satisfy the Definition 1 in general.

For a general configuration $g \in \mathrm{SE}(2)$ in (6), it can be decomposed into the following form:

$$g = \begin{bmatrix} R(\theta_c) & \begin{bmatrix} x \\ y \end{bmatrix} \\ 0_{1\times 2} & 1 \end{bmatrix} \begin{bmatrix} R(\triangle\theta) & \begin{bmatrix} 0 \\ 0 \end{bmatrix} \\ 0_{1\times 2} & 1 \end{bmatrix} = g_c\exp\{(\xi_{\triangle\theta})^\wedge\} \tag{10}$$

where $\triangle\theta = \theta - \theta_c$ and $\xi_{\triangle\theta} = [\triangle\theta, 0, 0]^T$. Then, (10) implies that

$$g_c^{-1}g = \exp\{(\xi_{\triangle\theta})^\wedge\}. \tag{11}$$

From the abovementioned observation, one can summarize the following proposition.

Proposition 2: If the heading angle θ in (6) converges to the c-nonholonomic trajectory's heading angle θ_c (i.e., $\triangle\theta \to 0$), then the configuration $g \in \mathrm{SE}(2)$ in (6) reduces to the c-nonholonomic trajectory, i.e., $g \in \mathcal{G}_c$.

Based on the analysis of c-nonholonomic trajectory, which provides a novel approach to achieve the arbitrary configuration stabilization, the global discontinuous time-invariant feedback

controller with input saturation will be designed in the following section.

IV. Controller Design and Stability Analysis

In this section, by following the c-nonholonomic trajectory approach, we first solve the arbitrary configuration stabilization problem with input saturation. Then, based on the stabilization controller, the automatic parking application with approximate desired trajectory in practice is analyzed.

A. Arbitrary Configuration Stabilization

The relative configuration between the desired configuration g_d and the real-time configuration g is denoted as $g_e = g_d^{-1}g$. Then, the relative position and attitude angle of relative configuration g_e are denoted by $p_e = [x_e, y_e]^T$ and $\theta_e \in (-\pi, \pi]$.

Based on the proposed c-nonholonomic trajectory approach and its property in Section III, a c-nonholonomic attitude α is designed as follows:

$$\alpha = \beta \arctan(y_e/x_e). \tag{12}$$

In order to avoid undesired equilibrium point, we define that $\beta \neq 2Z$ in the set $(x_e = 0, y_e \neq 0, \theta_e \in (-\pi, \pi])$, otherwise $\beta = 2$. To proceed, the attitude error between α and θ_e is defined as

$$\alpha_e = \theta_e - \alpha \tag{13}$$

where $\theta_e \in (-\pi, \pi]$. Based on the defined attitude error α_e and (1), one can obtain the following equation:

$$\dot{\alpha}_e = \omega - \dot{\alpha} \tag{14a}$$

$$\dot{x}_e = v \cos\theta_e \tag{14b}$$

$$\dot{y}_e = v \sin\theta_e. \tag{14c}$$

In the following, the main objective is to design the control law to stabilize the kinematic equation (14). To ensure that the designed linear speed and angular speed are saturated, we propose the following control function:

$$v = -k_1 \tanh(x_e \cos\theta_e + y_e \sin\theta_e) \tag{15a}$$

$$\omega = -k_2 \tanh(\alpha_e) + \dot{\alpha} \tag{15b}$$

where k_1, k_2 are positive constants which satisfy the following inequalities:

$$k_1 \leq v_m, |k_1 + k_2| \leq \omega_m, |k_1 - k_2| \leq \omega_m. \tag{16}$$

Before giving the main results, the following lemma is first proposed.

Lemma 4: For any given $x \in \mathbb{R}, y \in \mathbb{R}, \theta \in (-\pi, \pi]$ with $x^2 + y^2 \neq 0$, the following inequality holds:

$$-\frac{1}{2} \leq \frac{(x\cos\theta + y\sin\theta)(x\sin\theta - y\cos\theta)}{x^2 + y^2} \leq \frac{1}{2}. \tag{17}$$

Proof: Denote $a = x\cos\theta + y\sin\theta$, and $b = x\sin\theta - y\cos\theta$. Then, the equality $a^2 + b^2 = x^2 + y^2$ holds. Using $(a-b)^2 = a^2 - 2ab + b^2 \geq 0$, one has $ab \leq \frac{1}{2}(a^2 + b^2)$, which implies that the inequality $\frac{ab}{a^2+b^2} \leq \frac{1}{2}$ holds. On the other hand, from $(a+b)^2 = a^2 + 2ab + b^2 \geq 0$, one obtains $ab \geq -\frac{1}{2}(a^2 + b^2)$, which implies that the inequality $-\frac{1}{2} \leq \frac{ab}{a^2+b^2}$ holds. Thus, the inequality (17) holds. ■

Now, the following theorem summarizes the arbitrary configuration stabilization result of nonholonomic vehicles with local measurements on vehicle body-fixed frames.

Theorem 1: Consider the nonholonomic vehicle (1) with the desired constant configuration $g_d \in \mathrm{SE}(2)$. The arbitrary configuration stabilization problem (i.e., $\lim_{t\to\infty} g_e \to I_3$) with input saturation (2) is solved by the saturated control input (15) with the gains satisfying (16).

Proof: First, we prove that the designed control input (15) is saturated. If $k_1 \leq v_m$, the linear speed v in (15a) is saturated obviously. Furthermore, based on inequality (17), $|\dot{\alpha}|$ can be calculated as

$$\begin{aligned}|\dot{\alpha}| &= 2\frac{|v(x_e\sin\theta_e - y_e\cos\theta_e)|}{x_e^2 + y_e^2} \\ &= 2k_1\frac{|\tanh(x_e\cos\theta_e + y_e\sin\theta_e)(x_e\sin\theta_e - y_e\cos\theta_e)|}{x_e^2 + y_e^2} \\ &\leq 2k_1\frac{|(x_e\cos\theta_e + y_e\sin\theta_e)(x_e\sin\theta_e - y_e\cos\theta_e)|}{x_e^2 + y_e^2} \leq k_1.\end{aligned} \tag{18}$$

Thus, the inequality $|k_2 - k_1| \leq ||-k_2\sin\alpha_e| - |\dot{\alpha}|| \leq |\omega| \leq ||-k_2\sin\alpha_e| + |\dot{\alpha}|| \leq |k_2 + k_1|$ holds. If the gains satisfy (16), the input saturation objective (2) is guaranteed.

Second, consider the following positive definite Lyapunov function:

$$V = \frac{1}{2}x_e^2 + \frac{1}{2}y_e^2 + \frac{1}{2}\alpha_e^2 \tag{19}$$

Its time derivative along the trajectory (14) with the control input (15) is given by

$$\begin{aligned}\dot{V} = &-k_1(x_e\cos\theta_e + y_e\sin\theta_e)\tanh(x_e\cos\theta_e + y_e\sin\theta_e) \\ &-k_2\alpha_e\tanh(\alpha_e) \leq 0\end{aligned} \tag{20}$$

where the properties of $x\tanh(x) \geq 0$ is used. Hence, as $t \to \infty$, the closed-loop system is stable, which implies that

$$(x_e\cos\theta_e + y_e\sin\theta_e) = 0, \quad \theta_e = \alpha. \tag{21}$$

Thus, the states x_e, y_e, θ_e converge to the following set:

$$\mathcal{M} = \{(x_e, y_e, \theta_e) | x_e\cos\theta_e = -y_e\sin\theta_e, \theta_e = \alpha\}. \tag{22}$$

Denote the set $\mathcal{L}$ as the largest invariant set contained in the set $\mathcal{M}$. According to the equilibrium condition in equation (21), the set $\mathcal{M}$ can be divided into the following seven cases to derive the largest invariant set $\mathcal{L}$.

Case 1: $y_e = 0$ and $\sin\theta_e = 0$. From (21), one has $x_e = 0$ or $\cos\theta_e = 0$. If $x_e = 0$, one concludes that $\alpha = \theta_e = 0$, and an element in the set $\mathcal{L}$ is $(x_e, y_e, \theta_e) = (0, 0, 0)$. If $\cos\theta_e = 0$, one has $\theta_e = \pm\frac{\pi}{2} = \alpha$ since $\theta_e \in (-\pi, \pi]$. However, from (12), $\alpha = \pm\frac{\pi}{2}$ contradicts with $y_e = 0$. Thus, in this case, the largest invariant set $\mathcal{L}$ only contains the solution $(x_e, y_e, \theta_e) = (0, 0, 0)$.

Case 2: $y_e \neq 0$ and $\sin\theta_e = 0$. Since $\theta_e \in (-\pi, \pi]$, in this case, $\theta_e = \pi = \alpha$ or $\theta_e = 0 = \alpha$. Combined with (21), one has $x_e = 0$ and $\cos\theta_e \neq 0$. Under the condition $y_e \neq 0, x_e = 0$ in (12), one has $\alpha = \pm\frac{\pi}{2}\beta$, which contradicts with $\alpha = \pi$, where

$\beta \neq 2Z$ is used. If $\theta_e = \alpha = 0$, then y_e contradicts with $y_e \neq 0$. Thus, this case does not hold.

Case 3: $y_e = 0$ and $\sin\theta_e \neq 0$. From (21), one has $x_e = 0$ or $\cos\theta_e = 0$. From (12), $\theta_e = \alpha = 0$ if $x_e = 0$, which contradicts with $\sin\theta_e \neq 0$. In the case of $\sin\theta_e \neq 0$ and $\cos\theta_e = 0$, from $\theta_e \in (-\pi, \pi]$, one has $\theta_e = \pm\frac{\pi}{2}$, which contradicts with $y_e = 0$. Thus, this case does not hold.

Case 4: $x_e = 0$ and $\cos\theta_e = 0$. Since $\theta_e \in (-\pi, \pi]$, one has $\theta_e = \pm\frac{\pi}{2} = \alpha$. Combined with (21), one has $y_e = 0$. However, from (12), $\alpha = \pm\frac{\pi}{2}$ contradicts with $y_e = 0$. Thus, this case does not hold.

Case 5: $x_e \neq 0$ and $\cos\theta_e = 0$. Since $\theta_e \in (-\pi, \pi]$, one has $\theta_e = \pm\frac{\pi}{2} = \alpha$. Combined with (21), one has $y_e = 0$. If $y_e = 0$, one has $\alpha = 0$ which contradicts with $\cos\theta_e = \cos\alpha = 0$. Thus, this case does not hold.

Case 6: $x_e = 0$ and $\cos\theta_e \neq 0$. From (21), one has $y_e = 0$ or $\sin\theta_e = 0$. If $y_e = 0$, one obtains that $\alpha = 0 = \theta_e$, and $(x_e, y_e, \theta_e) = (0, 0, 0)$ in the set $\mathcal{L}$. If $\sin\theta_e = 0$ and $y_e \neq 0$, it can be excluded by Case 2. Thus, in this case, the largest invariant set $\mathcal{L}$ only contains the desired equilibrium point $(x_e, y_e, \theta_e) = (0, 0, 0)$.

Case 7: $x_e \neq 0$, $y_e \neq 0$, $\sin\theta_e \neq 0$ and $\cos\theta_e \neq 0$. From (21), one obtains the following equality:

$$\frac{\cos\theta_e}{\sin\theta_e} = -\frac{y_e}{x_e} = -\tan\left(\frac{\alpha}{2}\right). \tag{23}$$

Furthermore, based on (23), one has the following equality:

$$\tan(\theta_e)\tan\left(\frac{\alpha}{2}\right) = \frac{-(\cos(\frac{\alpha}{2}+\theta_e) - \cos(\frac{\alpha}{2}-\theta_e))}{\cos(\frac{\alpha}{2}+\theta_e) + \cos(\frac{\alpha}{2}-\theta_e)} = -1. \tag{24}$$

Then, the abovementioned equation can be rewritten as

$$\cos\left(\frac{\alpha}{2} - \theta_e\right) = -\cos\left(\frac{\alpha}{2} - \theta_e\right) \tag{25}$$

which implies that

$$\cos\left(\frac{\alpha}{2} - \theta_e\right) = 0. \tag{26}$$

Thus, one obtains that

$$\frac{\alpha}{2} - \theta_e = \frac{\pi}{2} + Z\pi. \tag{27}$$

Since $\theta_e = \alpha$ in (21), one obtains that

$$\alpha = \theta_e = (2Z - 1)\pi \tag{28}$$

which contradicts with $\sin\theta_e \neq 0$. Thus, this case does not hold.

By summing up Cases 1–7, the largest invariant set $\mathcal{L}$ contains only the desired equilibria $(x_e, y_e, \theta_e) = (0, 0, 0)$. Thus, based on the LaSalle's invariance theorem [33], the proof is finished.■

Remark 2: Note that the gain of $\arctan(y_e/x_e)$ in (12) is denoted as $\beta = 2$ except the set $(x_e = 0, y_e \neq 0, \theta_e \in (-\pi, \pi])$. The reasons are explained as follows. First, as discussed in Section III, $\alpha = 2\arctan(y_e/x_e)$ is an attitude, which satisfies the c-nonholonomic trajectory. Second, from the analysis in (26) and (27), by choosing the gain $\beta = 2$, Case 7 could be excluded in the proof of Theorem 1. Furthermore, in the set $(x_e = 0, y_e \neq 0, \theta_e \in (-\pi, \pi])$, there exists an undesired equilibrium point $(x_e = 0, y_e \neq 0, \theta_e = \pi)$. If the trajectory starts on or enters the undesired equilibrium, the gain $\beta \neq 2Z$ implies that the trajectory escapes the set $(x_e = 0, y_e \neq 0, \theta_e \in (-\pi, \pi])$. Thus, from the well-known Brockett's theorem, the proposed time-invariant state feedback stabilization control law is discontinuous.

Remark 3: It is worth pointing out that the c-nonholonomic trajectory cannot be established if the initial configuration is chosen as $(x_e(0) \neq 0, y_e(0) = 0, \theta_e(0) \in (-\pi, \pi])$. To deal with this and ensure the global convergence, the function $\tanh(\cdot)$ is used in (15b), which enables the trajectory to escape from those configurations and find the feasible c-nonholonomic trajectory. In practice, except for the configurations $(x_e(t) \neq 0, y_e(t) = 0, \theta_e(t) \in (-\pi, \pi])$, the function $\sin(\cdot)$ should be used in the angular speed, and is designed as

$$\omega = -k_2 \sin\alpha_e + \dot{\alpha}. \tag{29}$$

The function $\sin\alpha_e$ helps avoiding the unwinding phenomenon. For example, by choosing $\alpha = -3$rad, and $\theta_e = 3$rad, the function $-k_2\sin(\theta_e - \alpha) = -k_2\sin(6) > 0$ indicates that the vehicle rotates the clockwise direction with a small rotation in achieving the tracking goal, while the function $-k_2\tanh(\theta_e - \alpha) = -k_2\tanh(6) < 0$ implies the vehicle rotates the anticlockwise direction, which causes the unnecessary rotation. Thus, in the feasible trajectory, the angular speed (29) has a better transient performance.

Remark 4: In practice, the saturated input plays a very important role. In fact, due to physical limitations (e.g., the maximum allowable linear and angular velocity inputs) of the vehicle [17], [18], a theoretically designed control function may exceed the limits and becomes infeasible in implementation. Different from the stabilization control for nonholonomic vehicles that uses other auxiliary attitude methods to achieve the simultaneous position and attitude stabilization that does not ensure a saturated input [20]–[22], [24], [25], the designed controller in this paper guarantees the desired input saturation to meet practical implementation requirement.

Remark 5: The simultaneous stabilization and tracking controller can be designed as extensions from the proposed arbitrary configuration stabilization controller, and readers could refer to [24]. However, there are some difficulties to extend the controller to simultaneously achieve the stabilization and tracking with input saturation, which will be a challenging topic in the future research.

Remark 6: From the practice point of view, we expect that the heading of a nonholonomic vehicle could satisfy the attitude of c-nonholonomic trajectory as soon as possible, so that the vehicle could move along the desired c-nonholonomic trajectory. An application scenario in automatic parking described in the next Section IV-B illustrates this property. Thus, in practice, the gain k_2 should be chosen a bit larger than the gain k_1.

B. Applications to Automatic Parking With an Approximate Desired Trajectory

Compared to the previous simultaneous position and attitude controllers in [19]–[22] and [24]–[27], the designed stabilization controller not only guarantees the input saturation, but also has

good foreground on automatic parking scenario. In the context of automatic parking for nonholonomic vehicles, the definition of automatic parking with an approximate desired trajectory is defined as follows.

Definition 3: Automatic parking with an approximate desired trajectory refers to that the nonholonomic vehicle could calculate a motion curve from the initial and desired configurations in advance, and the vehicle runs in a region near the calculated trajectory.

Based on the analysis of Proposition 2, the designed velocity input (15) plays an important role in tuning the vehicle's heading towards the c-nonholonomic trajectory. With the designed angular speed, the heading of the nonholonomic vehicle is controlled to reach the attitude of the c-nonholonomic trajectory, so that the attitude error α_e reaches and remains zero (i.e., $\theta = \alpha$). Using $\alpha_e = 0$, one obtains that $\dot{\alpha}_e = \omega - \dot{\alpha} = 0$, which implies that $\omega = \dot{\alpha}$. The time derivative of α is given as follow:

$$\omega = \dot{\alpha}(t) = \frac{2v(t)(x_e(t)\sin\theta_e(t) - y_e(t)\cos\theta_e(t))}{x_e(t)^2 + y_e(t)^2}. \quad (30)$$

Thus, the radius of the nonholonomic vehicle trajectory is

$$r(t) = \left|\frac{v(t)}{\omega(t)}\right| = \left|\frac{x_e(t)^2 + y_e(t)^2}{2(x_e(t)\sin\theta_e(t) - y_e(t)\cos\theta_e(t))}\right|. \quad (31)$$

Regarding the radius (31), the following proposition holds.

Proposition 3: The radius of the nonholonomic vehicle trajectory in (31) is a positive constant when the attitude error $\alpha_e = 0$ holds.

Proof: Consider the positive definite Lyapunov function $W = 1 - \cos\alpha_e$. Using the angular speed input (29), one has $\dot{W} = -k_2 \sin^2\alpha_e \leq 0$. Thus, from Lemma 3, one concludes that the trajectory satisfies the definition of c-nonholonomic trajectory after the angle reaches $\theta_e = \alpha$. Since then, at any time moment, the c-nonholonomic trajectory will hold. According to $x_e = \bar{c}\sin\theta_e$ and $y_e = \bar{c}(1 - \cos\theta_e)$ in Definition 1, (31) can be rewritten as

$$r(t) = \left|\frac{(\bar{c}\sin\theta_e)^2 + (\bar{c}(1-\cos\theta_e))^2}{2(\bar{c}\sin^2\theta_e - \bar{c}(1-\cos\theta_e)\cos\theta_e)}\right| = \bar{c} \quad (32)$$

where $\bar{c}$ is a positive constant at any time t after $\theta_e = \alpha$. Thus, (32) implies that $r(t) = \bar{c}$ is a positive constant after $\theta_e = \alpha$.■

The magnitude of $r(t)$ in (31) depends on the state error when the attitude of nonholonomic vehicle converges to the desired attitude that satisfies the definition of c-nonholonomic trajectory. In practice, the heading of the nonholonomic vehicle is controlled to converge to the desired heading in a short time duration under a suitable gain k_2, and the initial state error $x_e(0), y_e(0), \theta_e(0)$ changes mildly when the trajectory satisfies the defined c-nonholonomic trajectory. From this point of view, the radius $r(t)$ of the c-nonholonomic trajectory can be calculated by the initial configuration. Based on the analysis of Lemma 3, the approximate desired trajectory is a part of circle with the radius (33) approximated by the following formula:

$$r \approx \left|\frac{x_e(0)^2 + y_e(0)^2}{2y_e(0)}\right| \quad (33)$$

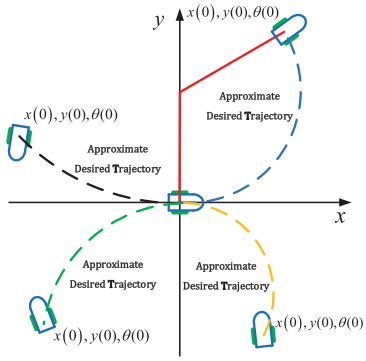

Fig. 2. Illustrations of different approximate desired trajectories.

and the center of circle motion is given as

$$\begin{bmatrix} x_c \\ y_c \end{bmatrix} = \begin{bmatrix} \cos\theta_d & -\sin\theta_d \\ \sin\theta_d & \cos\theta_d \end{bmatrix} \begin{bmatrix} 0 \\ r \end{bmatrix}. \quad (34)$$

Thus, based on the abovementioned analysis and Definition 3, the actual trajectory will move within the region close to the trajectory calculated by (33) and (34). It is worth to mention that, in practice, the approximate desired trajectory can be calculated in advance according to the planning of initial configurations, which help to enhance obstacle avoidance in the automatic parking scenario. Without loss of generality, let the desired configuration be the origin of inertial frame, i.e., $g_d = I_3$, and the approximate desired trajectory is shown in Fig. 2.

If the initial configuration and the desired configuration are relatively close, the trajectories of nonholonomic vehicle will consist of many different c-nonholonomic trajectories. Although it does not look like a c-nonholonomic trajectory, the actual trajectory also satisfies conditions of an approximate desired trajectory. Those properties will be presented in the numerical simulations.

Remark 7: From Proposition 3, one knows that the trajectory of the nonholonomic vehicle is a circle with a constant radius after $\theta_e = \alpha$, and the c-nonholonomic trajectory can be guaranteed. To maintain an almost constant radius during some time interval, the linear speed can be the maximum v_m or $-v_m$, while the angular speed is small under the input saturation and equation $r = v/\omega$.

Remark 8: Based on the proposed controller, the vision-based control structure can be achieved since $R_d^T(p - p_d) = -(R^T R_d)^T(R^T(p_d - p))$, where $R^T(p_d - p)$ is the relative position measurements of a desired position in the vehicle's body-fixed frame. Thus, the proposed control algorithm does not require the Global Positioning System, which facilitates the control implementation in practice.

V. Numerical Simulation and Experiment

A. Numerical Simulation

Numerical simulations are provided in this section to verify the performance and effectiveness of the designed control algorithm. The initial configurations of four cases are presented as

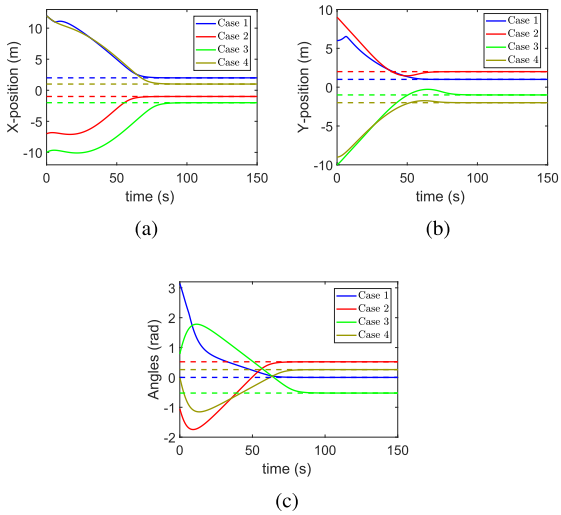

Fig. 3. Evolutions of x-position, y-position, and angles in the numerical simulation, where the solid line represents the real trajectory, and the dashed line represents the desired trajectory. (a) X-position (m). (b) Y-position (m). (c) Headings (rad).

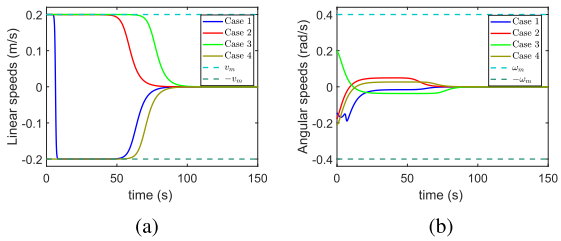

Fig. 4. Evolutions of linear speeds and angular speeds in the numerical simulation, where the solid line represents the real trajectory, and the dashed line represents the desired trajectory. (a) Linear speeds (m/s). (b) Angular speeds (rad/s).

follows:

$$\begin{aligned}
&\text{Case 1}: g = (\pi, 12, 6), && g_d = (0, 2, 1)\\
&\text{Case 2}: g = (-\pi/3, -7, 9), && g_d = (\pi/6, -1, 2)\\
&\text{Case 3}: g = (\pi/4, -10, -10), && g_d = (-\pi/6, -2, -1)\\
&\text{Case 4}: g = (0, 12, -9), && g_d = (\pi/12, 1, -2).
\end{aligned}$$

The maximum linear speed and angular speed are set as $v_m = 0.2$ m/s, and $\omega_m = 0.4$ rad/s. Thus, the control gains of four cases are all chosen as $k_1 = 0.2$ and $k_2 = 0.2$.

Based on the designed control law (15) and (29), the evolution of system states in four cases is described in Fig. 3, which shows that all system states in four cases converge to the desired states. The evolution of linear speeds and angular speeds is depicted in Fig. 4, from which one sees that the input saturation is guaranteed with the proposed c-nonholonomic trajectory approach. The vehicles' trajectories of four cases in the two-dimensional space are plotted in Fig. 5, which not only illustrates the effectiveness of the c-nonholonomic trajectory approach proposed in Section III, but also demonstrates the automatic parking application scenario

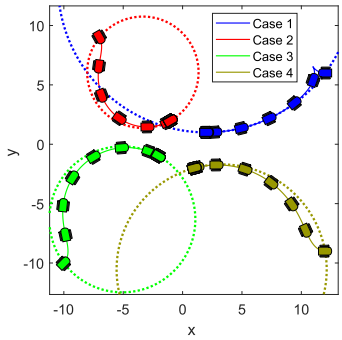

Fig. 5. Trajectories of each vehicle in the numerical simulation, where the dashed line represents the desired trajectory, which is a circle trajectory.

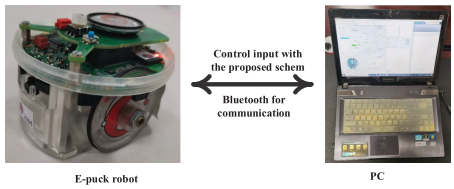

Fig. 6. Experimental platform.

discussed in Section IV-B that the real trajectory moves in the area near the desired trajectory.

B. Experiment

To demonstrate the applicability of the proposed control scheme in real applications, we perform an experiment on a physical robotic system and present the experiment verification results in this section. The experimental platform uses one nonholonomic robot named the wheeled E-puck robot [2], [29], where the experimental setup is shown in Fig. 6. In this experiment, the sampling period time via Bluetooth communication is chosen as 0.3 s. The E-puck robot is modeled with a unicycle-like dynamics, while we denote v_L and v_R the speeds of the left and right wheels with the limitation $v_{L/R} \leq a$, where a is the wheel speed limited by $a = 0.13$ m/s. Noting that $v = (v_R + v_L)/2$, and $\omega = (v_R - v_L)/2b$, where $b = 0.0267$ m is the wheel base, the E-puck robot has the limitation that $\frac{|v|}{a} + \frac{b|\omega|}{a} \leq 1$. Due to the abovementioned limitations, we choose $k_1 = 0.1$ and $k_2 = 0.15$ in the experiment. The initial configuration is set as $g(0) = (\pi \text{ rad}, 0 \text{ m}, 0 \text{ m})$, and the desired configuration is defined as $g_d = (0 \text{ rad}, 1.6 \text{ m}, 2.4 \text{ m})$. The evolutions of vehicles' positions and headings are plotted in Fig. 7, and the linear speed and angular speed of the robot are presented in Fig. 8 (plotted by MATLAB with sampled data from the experiments). Besides, Fig. 9 shows the real-time trajectories of the robot in the platform, which are captured by a video camera. We refer the readers to the attached video for real time trajectories. From the experiment results, it further validates the effectiveness of the proposed arbitrary configuration stabilization control scheme based on a c-nonholonomic trajectory and its applications in vehicle automatic parking with an approximate desired trajectory.

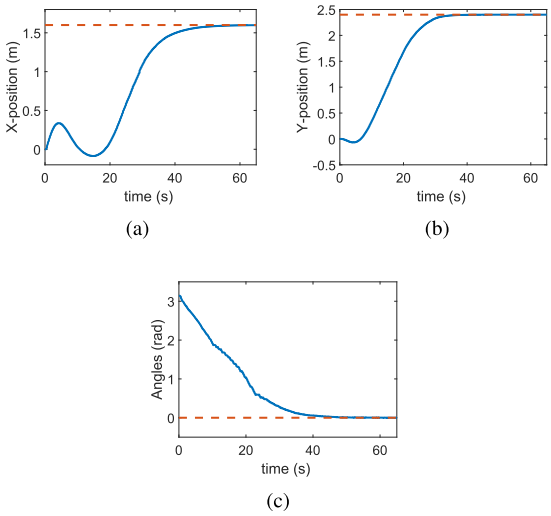

Fig. 7. Evolutions of x-position, y-position, and angle in the experiment. (a) X-position (m). (b) Y-position (m). (c) Headings (rad).

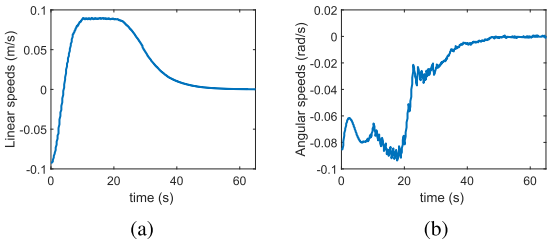

Fig. 8. Evolutions of linear speeds and angular speeds in the experiment. (a) Linear speeds (m/s). (b) Angular speeds (rad/s).

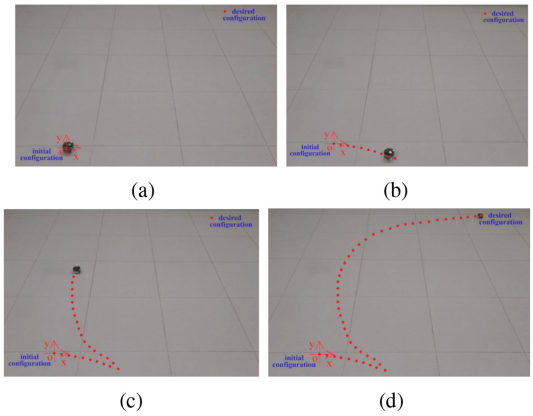

Fig. 9. Trajectories of the E-puck robot in the experiment, with $t = 0$ s, $t = 9$ s, $t = 25$ s, $t = 60$ s. (a) $t = 0$ s. (b) $t = 9$ s. (c) $t = 25$ s. (d) $t = 60$ s.

VI. Conclusion

In this article, the arbitrary configuration stabilization control with input saturation for nonholonomic vehicles and its application in automatic parking was investigated. We first proposed a novel definition of c-nonholonomic configuration, and discover its c-nonholonomic trajectory properties. Based on the proposed c-nonholonomic trajectory approach, the arbitrary configuration stabilization control problem was solved under input saturation. The motion behavior with the proposed control law was analyzed, and the application in automatic parking was addressed. Both numerical simulations and experiments were provided to illustrate the performance of the proposed control approach.

References

[1] K. D. Do and J. Pan, "Nonlinear formation control of unicycle-type mobile robots," *Robot. Auton. Syst.*, vol. 55, no. 3, pp. 191–204, Mar. 2007.
[2] Z. Sun, Y. Xia, L. Dai, K. Liu, and D. Ma, "Disturbance rejection MPC for tracking of wheeled mobile robot," *IEEE/ASME Trans. Mechatronics*, vol. 22, no. 6, pp. 2576–2587, Dec. 2017.
[3] J. Wang, G. Wen, Z. Duan, and J. Lü, "Stochastic consensus control integrated with performance improvement: A consensus region-based approach," *IEEE Trans. Ind. Electron.*, vol. 67, no. 4, pp. 3000–3012, Apr. 2020.
[4] Q. Wang, Z. Duan, Y. Lv, Q. Wang, and G. Chen, "Distributed model predictive control for linear-quadratic performance and consensus state optimization of multi-agent systems," *IEEE Trans. Cybern.*, to be published, doi: 10.1109/TCYB.2020.3001347.
[5] R. W. Brockett, "Asymptotic stability and feedback stabilization," in *Differential Geometric Control Theory*, R. W. Brockett, R. S. Millman, and H. J. Sussmann. Boston, MA, USA: Birkhauser, 1983, pp. 181–191.
[6] Z. Jiang and H. Nijmeijer, "Tracking control of mobile robots: A case study in backstepping," *Automatica*, vol. 33, no. 7, pp. 1393–1399, Jul. 1997.
[7] W. E. Dixon, Z. Jiang, and D. M. Dawson, "Global exponential set-point control of wheeled mobile robots: A Lyapunov approach," *Automatica*, vol. 36, no. 11, pp. 1741–1746, Nov. 2000.
[8] Y. Y. Aye, K. Watanabe, S. Maeyama, and I. Nagai, "Invariant manifold-based stabilizing controllers for nonholonomic mobile robots," *Artif. Life Robot.*, vol. 20, no. 3, pp. 276–284, Oct. 2015.
[9] Y. Tian and S. Li, "Exponential stabilization of nonholonomic dynamic systems by smooth time-varying control," *Automatica*, vol. 38, no. 7, pp. 1139–1146, Jul. 2002.
[10] C. C. de Wit and O. J. Sordalen, "Exponential stabilization of mobile robots with nonholonomic constraints," *IEEE Trans. Autom. Control*, vol. 13, no. 11, pp. 1791–1797, Nov. 1992.
[11] A. Bloch, M. Reyhanoglu, and N. H. McClamroch, "Control and stabilization of nonholonomic dynamic systems," *IEEE Trans. Autom. Control*, vol. 37, no. 11, pp. 1746–1757, Nov. 1992.
[12] T. Urakubo, "Feedback stabilization of a nonholonomic system with potential fields: Application to a two-wheeled mobile robot among obstacles," *Nonlinear Dyn.*, vol. 81, no. 3, pp. 1475–1487, Aug. 2015.
[13] O. J. Sordalen and O. Egeland "Exponential stabilization of nonholonomic chained systems," *IEEE Trans. Autom. Control*, vol. 40, no. 1, pp. 35–49, Jan. 1995.
[14] B. Mu, J. Chen, Y. Shi, and Y. Chang, "Design and implementation of nonuniform sampling cooperative control on a group of two-wheeled mobile robots," *IEEE Trans. Ind. Electron.*, vol. 64, no. 6, pp. 5035–5044, Jun. 2017.
[15] I. Kolmanovsky and N. H. McClamroch, "Stabilization of nonholonomic Chaplygin systems with linear base space dynamics," in *Proc. 34th IEEE Conf. Decis. Control*, Dec. 1995, pp. 27–32.
[16] P. Morin, and C. Samso, "Control of nonholonomic mobile robots based on the transverse function approach," *IEEE Trans. Robot*, vol. 25, no. 5, pp. 1058–1073, Oct. 2009.
[17] J. Fu, G. Wen W. Yu, T. Huang, and X. Yu, "Consensus of second-order multiagent systems with both velocity and input constraints," *IEEE Trans. Ind. Electron*, vol. 66, no. 10, pp. 7946–7955, Oct. 2019.
[18] J. Fu, Y. Lv, and T. Huang, "Distributed anti-windup approach for consensus tracking of second-order multi-agent systems with input saturation," *Syst. Control Lett.*, vol. 130, pp. 1–6, 2019.
[19] J. Huang, C. Wen, W. Wang, and Z. Jiang, "Adaptive stabilization and tracking control of a nonholonomic mobile robot with input saturation and disturbance," *Syst. Control Lett.*, vol. 62, no. 3, pp. 234–241, Mar. 2013.
[20] Y. Wang, Z. Miao, H. Zhong, and Q. Pan, "Simultaneous stabilization and tracking of nonholonomic mobile robots: A Lyapunov-based approach," *IEEE Trans. Control Syst. Technol.*, vol. 23, no. 4, pp. 1440–1450, Jul. 2015.
[21] Z. Miao and Y. Wang, "Adaptive control for simultaneous stabilization and tracking of unicycle mobile robots," *Asian J. Control*, vol. 17, no. 6, pp. 2277–2288, 2015.

[22] M. Maghenem, A. Loria, and E. Panteley, "Cascades-based leader-follower formation-tracking and stabilization of multiple nonholonomic vehicles," *IEEE Trans. Autom. Control*, vol. 63, no. 8, pp. 2662–2669, Aug. 2018.
[23] D. Panagou and K. J. Kyriakopoulos, "Viability control for a class of underactuated systems," *Automatica*, vol. 49, no. 1, pp. 17–29, Jan. 2013.
[24] M. Tayefi and Z. Geng, "Logarithmic control, trajectory tracking, and formation for nonholonomic vehicles on lie group SE(2)," *Int. J. Control*, Vol. 92, no. 1, pp. 204–224, 2019.
[25] X. He and Z. Geng, "Arbitrary point-to-point stabilization control in specified finite time for wheeled mobile robots based on dynamic model," *Nonlinear Dyn.*, vol. 97, pp. 937–954, May 2019.
[26] T.-C. Lee, K.-T. Song, C.-H. Lee, and C.-C. Teng, "Tracking control of unicycle-modeled mobile robots using a saturation feedback controller," *IEEE Trans. Control Syst. Technol.*, vol. 9, no. 2, pp. 305–318, Mar. 2001.
[27] Z. Wang, G. Li, X. Chen, H. Zhang, and Q. Chen, "Simultaneous stabilization and tracking of nonholonomic WMRs with input constraints: Controller design and experimental validation," *IEEE Trans. Ind. Electron*, vol. 66, no. 7, pp. 5343–5352, Jul. 2019.
[28] X. Yu and L. Liu, "Distributed formation control of nonholonomic vehicles subject to velocity constraints," *IEEE Trans. Ind. Electron*, vol. 63, no. 2, pp. 1289–1298, Feb. 2016.
[29] X. Peng, Z. Sun, K. Guo, and Z. Geng, "Mobile formation coordination and tracking control for multiple nonholonomic vehicles," *IEEE/ASME Trans. Mechatronics* vol. 25, no. 3, pp. 1231–1242, Jun. 2020.
[30] F. Bullo and A. D. Lewis, *Geometric Control of Mechanical Systems*. New York, NY, USA: Springer, 2005.
[31] F. Bullo, and R. Murray, "Proportional derivative (PD) control on the euclidean group," in *Proc. Eur. Control Conf.*, Rome, Italy, 1995, pp. 1091–1097.
[32] A. Iserles, H. Z. Munthe-Kaas, S. P. Nørsett, and A. Zanna, "Lie group methods," *Acta Numerica*, vol. 9, pp. 215–365, 2000.
[33] H. K. Khalil, *Nonlinear Systems*. Upper Saddle River, NJ, USA: Prentice-Hall, 1996.

Xiuhui Peng received the B.S. degree in automatic control from Jiangnan University, Wuxi, China, in 2014, and the Ph.D. degree in mechanics and engineering science from Peking University, Beijing, China, in 2019.

He is currently a Lecturer with the College of Automation Engineering, Nanjing University of Aeronautics and Astronautics, Nanjing, China. His research interests include cooperative control, unmanned systems control, and nonlinear control of mechanical systems.

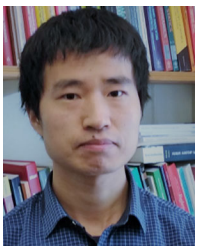

Zhiyong Sun (Member, IEEE) received the Ph.D. degree in control theory and engineering from The Australian National University (ANU), Canberra ACT, Australia, in Feb. 2017.

He was a Research Fellow/Lecturer with the Research School of Engineering, ANU, from 2017 to 2018. From June 2018 to January 2020, he was a Postdoctoral Researcher with the Department of Automatic Control, Lund University, Lund, Sweden. Since January 2020, he has been with the Eindhoven University of Technology (TU/e), The Netherlands, as an Assistant Professor. His research interests include multiagent systems, control of autonomous formations, and distributed optimization.

Dr. Sun was the recipient of the Australian Prime Ministers Endeavour Postgraduate Award in 2013 from the Australian Government, the Outstanding Oversea Student Award from the Chinese Government in 2016, and the Springer Ph.D. Thesis Prize from Springer in 2017. He was the recipient of the Best Student Paper Finalist Award from the 54th IEEE Conference on Decision and Control (2015), Osaka, Japan.

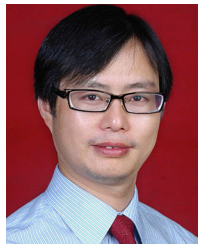

Mou Chen (Senior Member, IEEE) received the B.S. degree in material science and engineering and the Ph.D. degree in control theory and control engineering from the Nanjing University of Aeronautics and Astronautics, Nanjing, China, in 1998 and 2004, respectively.

He is currently a Full Professor with the College of Automation Engineering, Nanjing University of Aeronautics and Astronautics, China. He was an Academic Visitor with the Department of Aeronautical and Automotive Engineering, Loughborough University, U.K., from November 2007 to February 2008. From June 2008 to September 2009, he was a Research Fellow with the Department of Electrical and Computer Engineering, National University of Singapore. He was a Senior Academic Visitor with the School of Electrical and Electronic Engineering, The University of Adelaide, Australia, from May 2014 to November 2014. His research interests include nonlinear system control, intelligent control, and flight control.

Zhiyong Geng received the B.S. and M.S. degrees in engineering from Northeast University, Shenyang, China, in 1981 and 1984, respectively, and the Ph.D. degree in operational research and cybernetics from the Institute of Systems Science, Chinese Academy of Science, Beijing, China, in 1995.

From 1995 to 1997, he was a Postdoctoral Research Fellow with the Department of Mechanics and Engineering Science, Peking University, Beijing, where he is currently a Professor with the State Key Laboratory for Turbulence and Complex Systems and the Department of Mechanics and Engineering Science. His research interests include robust control and nonlinear control.